Periodica Polytechnica
Chemical Engineering

59(3), pp. 221-235, 2015
DOI: 10.3311/PPch.7577

RESEARCH ARTICLE

Study the Effect of Various Operating Parameters of Proton Exchange Membrane

Nima Ahmadi[1*], Sajad Rezazadeh[1], Iraj Mirzaee[1]

Received 21 June 2014; accepted after revision 20 October 2014

Abstract

A three-dimensional computational fluid dynamics in-house code to model the proton exchange membrane fuel cell (PEMFC) was developed. The equation was discretized and numerically solved by finite volume method and simple algorithm. In this research some parameters such as oxygen consumption, water production, temperature distribution, ohmic losses, anode water activity, cathode over potential and the fuel cell performance for straight single cell were investigated in more details. The numerical simulations reveal that these important operating parameters are highly dependent to each other and the fuel cell efficiency is affected by the kind of species distribution. So for especial uses in desirable voltages, for preventing from the unwilling losses, these numerical results can be useful. Also at the following an innovative gas flow channel design is introduced which named step-like gas channel. The numerical and experimental results indicate that new flow field design enhance cell performance significantly.

Finally the numerical results of proposed CFD model have been compared with the published experimental data that represent good agreement.

Keywords

PEM fuel cell, over-potential, water activity, Step-like, CFD

[1] Mechanical Engineering Department, Urmia University of Technology

[*] Corresponding author, e-mail: nima.ahmadi.eng@gmail.com

1 Introduction

In past decades, the researchers have tried to find the new technology as the solution to the energy and environmental problems [1-4]. In this way, they could gain the fuel cell technology.

The different types of fuel cells are distinguished by electrolyte used. Among them, the Proton Exchange Membrane Fuel Cell (PEMFC), which is focus of this paper, is described by the use of a polymer electrolyte membrane [5-9].

As shown in Fig. 1, a typical PEM fuel cell is consisting of 9 regions: anode (bipolar plate, gas channel, gas diffusion layer, and catalyst layer), membrane, cathode (bipolar plate, gas channel, gas diffusion layer, and catalyst layer).

The humidified air and hydrogen (to keep the membrane water swollen in order to enhance sufficient proton conductivity) enter the cathode and anode channels respectively. The hydrogen molecule diffuses through the anode diffusion layer towards the catalyst layer where divides into H^+ and electrons:

$$H_2 \longrightarrow 2H^+ + 2e^- \quad (1)$$

Since the membrane is considered impermeable for reactant gases and electrons, just protons can migrate through the membrane. The produced electrons travel through the conductive diffusion layer and an external circuit.

The main electro chemical reaction occurs on the cathode catalyst layer. The oxygen diffuses through the diffusion layer and reacts with the protons and electrons to form water and heat:

$$O_2 + 2H^+ + 2e^- \longrightarrow H_2O \quad (2)$$

Development of polymer membrane with high performance, thermal and water management is the subject that some studies have been focused on. If the membrane has good thermal and protonic conductivity, it can remain hydrated and can conduct the protons better [10]. On the other hand, some investigations have been focused on fuel cell structure design. These types of fuel cells have some advantages: low operating temperature (60-90 ºC), simple design, low weight and volume and the prospect of further significant cost reduction make PEMFC technology a candidate for transport applications as well as for small appliances such as laptop computers.

Although there are more advantages in using fuel cell technology, but still, current PEMFCs are considerably expensive than other power generation systems such as combustion engines and batteries. So it is critical to find a way to reduce cost and increase their power through engineering optimization. It requires a better understanding of PEMFCs and how various parameters affect their performance.

Some studies on fuel cells have been conducted experimentally and theoretically. Experimental studies of PEM fuel cells are prohibitive, so computer modeling is more cost effective and easier to important when design changes are made [11,12].

In the past, to provide understanding about fuel cell performance, numerical and theoretical fuel cell modeling has been used extensively. Numerous researchers have focused on different aspects of the fuel cell:

Bernardi and Verbrugge [13,14] investigated a one-dimensional, isothermal which provides valuable information about the physics of the electro-chemical reactions and transport phenomena in the gas diffusion, catalyst and membrane layer.

Fuller and Newman [15] published a quasi-two-dimensional model of the MEA, which is based on concentration solution theory for the membrane and accounts for thermal effects.

Nguyen and White [16] proposed a two-dimensional and isothermal model. They considered water transport through membrane by the electro osmosis drag force as well as heat transfer from the solid phase to the gas phase along the flow channels.

Baschuk and Li [17] published a one-dimensional, steady-state model where they included the degree of water flooding in the gas-diffusion electrodes as a modeling parameter.

Gurau et al. [18] first used the methods of computational fluid dynamics for PEM Fuel Cell modeling. They developed a two dimensional, steady-state model of a whole fuel cell, i.e. both flow channels with the MEA in between. In their model, there was no interaction between gas and liquid phase of water.

The first three-dimensional modeling was done by Dutta et al. [19]. They obtained velocity, density and pressure contours in the gas diffusion layers. Their results showed that the current direction is drastically dependent on the mass transfer mechanism in the membrane electrode assembly.

N.Ahmadi et al. [20] used a CFD model to predict the effect of prominent GDL layers in the enhancement of the performance of the PEMFC.

N. Pourmahmoud et al. [21] presented the results of a numerical investigation, using a comprehensive three-dimensional, single phase, non-isothermal and parallel flow model of a PEM fuel cell with deflected membrane electrode assembly (MEA). This numerical research has concentrated on the deflection parameter that affects this type of fuel cell performance.

This article presents the results of a numerical and experimental investigation using a PEM fuel cell with straight channels. The main objective of this work is to explain the mass transport phenomena, temperature variation and current density distribution of base model (model with straight flow channels). The model equations are then solved by a numerical method based on finite volume method (FVM). The model findings are then validated with the in-house experimental data (which named experimental1) and Wang et al. data [22].

Model equations and assumptions:

The proposed model includes the following assumptions:

(1) The system operates under steady state condition.

(2) The flow regime in channels is supposed to be laminar for reactant gases because of low velocities gradient and eventually low Reynolds number.

(3) The increasing gas mixtures behave as ideal gas.

(4) The gas diffusion layers, catalyst layers and membrane are isotropic and homogeneous porous media, which asserts that the porosity is constant in the whole region of the gas diffusers.

(5) The membrane is considered impermeable for reactant gases.

Model equations

In this numerical simulation, a single domain model formation was used for governing equations. These equations consist of:

Continuity equation:

Electrodes are considered as a porous medium where reactant gases are distributed on catalyst layers. If ε is the porosity inside porous mediums:

$$\frac{\partial(\rho\varepsilon u)}{\partial x}+\frac{\partial(\rho\varepsilon v)}{\partial y}+\frac{\partial(\rho\varepsilon w)}{\partial z}=S_1 \tag{3}$$

where S_m is mass source term. In the flow channels, this term is zero, because there is no reaction, but in the catalyst layers is not zero due to reaction of reactant species:

$$S_{H_2}=-\frac{M_{H_2}}{2F}R_{an} \tag{4}$$

$$S_{O_2}=-\frac{M_{O_2}}{4F}R_{cat} \tag{5}$$

$$S_{H_2O}=-\frac{M_{H_2O}}{2F}R_{cat} \tag{6}$$

S_{H_2} and S_{O_2} are negative, because they are being consumed, but S_{H_2O} is positive due to its formation in catalyst layer.is F the Faraday constant and M is the molecular weight of species.

Momentum equation:

In porous electrodes and for Newtonian fluid, the momentum equation can be written as:

$$\nabla\cdot(\varepsilon\rho\vec{u}\vec{u})=-\varepsilon\nabla p+\nabla\cdot(\varepsilon\mu\nabla\vec{u})+S_{mom} \tag{7}$$

where $\vec{u}$, p, μ and S_{mom} are velocity vector, pressure, viscosity and momentum source term respectively. The S_{mom} is used to describe Darcy's drag for flow through porous gas diffusion layers and catalyst layers as:

$$S_{mom} = -\frac{\mu}{\beta}\vec{u} \tag{8}$$

β is the gas permeability inside the porous mediums.

Mass transfer equation:

The continuity equation in steady state conditions is written as follows:

$$\nabla \cdot (\rho\varepsilon\vec{u}y_i) = -\nabla \cdot \vec{J}_i + S_i \tag{9}$$

where y_i and J_i are mass fraction and diffusion mass flux vector respectively. S_i is mass source term which has been presented in Eqs. (4-6).

Fick's equation gives the diffusion mass flux vector:

$$\vec{J}_i = -\sum \rho D_{ij}^{eff} \nabla \vec{y}_i \tag{10}$$

Within porous electrodes, mass transfer equation changes to:

$$\nabla \cdot (\rho\varepsilon\vec{u}y_i) = \nabla \cdot (\rho\varepsilon D_{ij}^{eff} \nabla \vec{y}_i) + S_i \tag{11}$$

D_{ij}^{eff} is estimated from the:

$$D_{ij}^{eff} = D_{ij} \times \varepsilon^{1.5} \tag{12}$$

D_{ij} is diffusivity of species inside.

Energy equation:

The energy equation is given by:

$$\nabla \cdot (\rho\varepsilon\vec{u}\vec{T}) = \nabla \cdot (k_{eff} \nabla \vec{T}) = S_T \tag{13}$$

k_{eff} is the effective thermal conductivity which is calculated as volume average of solid and fluid conductivity in porous medium. S_T is source term and defined with the following equation:

$$S_T = I^2 R_{ohm} + h_{reaction} + h_{phase} \tag{14}$$

Since phase change in numerical simulation was not considered, so h_{phase} would be omitted. $h_{reaction}$ is the heat generated through the chemical reactions and R_{ohm} is defined as:

$$R_{ohm} = \frac{t_m}{\sigma_{mem}} \tag{15}$$

where t_m and σ_{mem} is thickness and protonic conductivity of membrane respectively.

$$\sigma_{mem} = \exp\left[1268\left(\frac{1}{303} - \frac{1}{T}\right)\right] \times (0{,}005139\lambda - 0{,}00326) \tag{16}$$

where water content in the membrane, λ, is defined as the number of water molecules per sulfonate group inside the membrane. The water content can be expressed as a function of the water activity, a, by the following equation:

$$\lambda = 0{,}3 + 6a[1 - \tanh(a - 0{,}5)] + 3{,}9\sqrt{a}\left[1 - \tanh\left(\frac{a - 0{,}89}{0{,}23}\right)\right] \tag{17}$$

where the activity, a, is calculated by:

$$a = \frac{C_w RT}{P_{sat}} = \frac{P_w}{P_{sat}} \tag{18}$$

P_w, P_{sat} are water vapor and saturation pressure respectively.

Charge conservation equation:

As mentioned before, electrons transfer through conductive solid phase and protons transport through the membrane. So two charge equations are needed:

$$\nabla \cdot (\sigma_{sol} \nabla \varnothing_{sol}) + R_{sol} = 0 \tag{19}$$

$$\nabla \cdot (\sigma_{mem} \nabla \varnothing_{mem}) + R_{mem} = 0 \tag{20}$$

σ_{sol} and σ_{mem} are electrical conductivity of electrodes and membrane (S/m) respectively. $\varnothing_{sol}$ and $\varnothing_{mem}$ is defined as potential of electron and proton. R_{sol} and R_{mem} are source terms (they are current density (A/m^3)). These terms are only defined in the catalyst layers:

For the solid phase:

$R_{sol} = -R_{an}$ (< 0) Anode side

$R_{sol} = -R_{cat}$ (> 0) Cathode side

For the membrane phase

$R_{mem} = -R_{an}$ (> 0) Anode side

$R_{mem} = -R_{cat}$ (< 0) Cathode side

The source terms are calculated using the Butler-Volmer equation:

$$R_{an} = J_{an}^{ref}\left(\frac{[H_2]}{[H_2]_{ref}}\right)^{\gamma_{an}}\left(e^{(\alpha_{an}F/RT)\eta_{an}} - e^{-(\alpha_{cat}F/RT)\eta_{cat}}\right) \tag{21}$$

$$Rcat = J_{cat}^{ref}\left(\frac{[O_2]}{[O_2]_{ref}}\right)^{\gamma_{cat}}\left(e^{-(\alpha_{cat}F/RT)\eta_{cat}} - e^{-(\alpha_{an}F/RT)\eta_{cat}}\right) \tag{22}$$

J^{ref} is reference exchange current density (A/m^2).

Water transport through membrane:

Water molecules in PEM fuel cell are transported via electro-osmotic drag due to the properties of polymer electrolyte membrane in addition to the molecular diffusion. H+ protons transport water molecules through the polymer electrolyte membrane and this transport phenomenon is called electro-osmotic drag. In addition to the molecular diffusion and electro-osmotic drag, water is also produced in the catalyst layers due to the electro chemical reaction.

The assumption of single phase model is used here. It means that water generated from the cathodic equation is in a vapor state.

Boundary condition:

Constant mass flow rate at the channel inlet and constant pressure condition at the channel outlet, the no-flux conditions are executed for mass, momentum, species and potential conservation equations at all boundaries expect for inlets and outlets of the anode and cathode flow channels. Figure 1 shows the other surface boundary conditions.

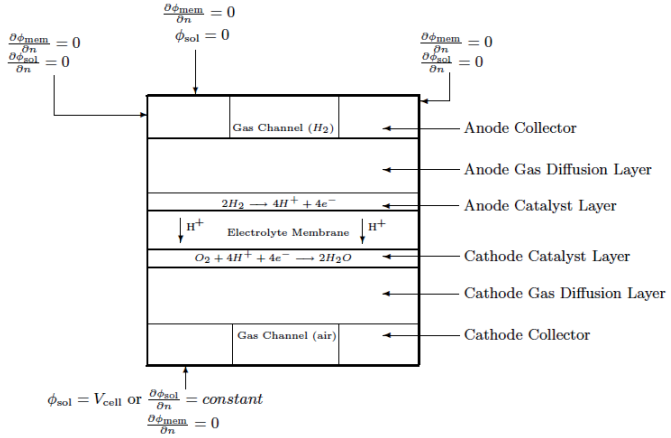

Fig. 1 Boundary conditions

Numerical and experimental implementation

For solving the equations, the SIMPLE algorithm [23] is applied. In addition the main procedure for discretizing the governing equations with the appropriate boundary conditions is finite volume method and implicit solver. Figure 2 shows the algorithm for numerical simulation of model's equations. For validating the numerical in-house code results, an empirical test set-up (1.2 kW) was established to obtain experimental results. Also all of in-house numerical and experimental results was compared to Wang et al. [22] data which shown good agreement.

In base model the structured meshes are used and in catalyst layers where the electro chemical reactions occur, the meshes are finer. Also grid independence test was implemented and finally the optimum number of meshes (174 000) chosen. Figure 3 indicates the computational domain of base model (which its components are listed in Fig. 1).

A series of simulation were carried out on the model from low to high operating current densities. In order to evaluate the validity of the model, numerical simulation results (for conventional model) compared with the experimental data presented by Wang et al. [22], as shown in Fig. 4, which there is a favorable agreement between them.

As it is clear from Fig. 4 there is a non-concurrence between the numerical simulation results and experimental data especially at high current density region. This fact is result of the single phase assumption. In other words, the water produced in the catalyst layer, is in the vapor phase (in numerical simulation). In fact, liquid water fills the pores of the catalyst and gas diffusion layers and do not let the oxygen molecules transfer to the catalyst layer easily. So the mass transfer resistance of reactants

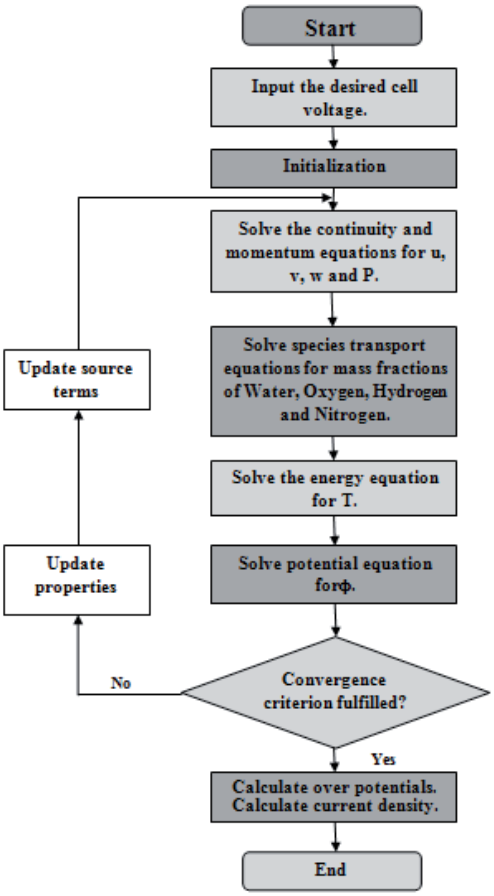

Fig. 2 Numerical implementation

(concentration loss) increases at high current density region. The power density curve for the model is illustrated too. There is a relation between voltage, current density and the power of the fuel cell as P =V.I.

Fuel cell operating condition and geometric parameters are shown in Table 1.

Table 1 Geometrical parameters and operating conditions

Parameter	value
Anode & Cathode pressure	3 atm
Anode & Cathode humidity	100%
Gas channel length	$Z=7.0\times10^{-2}$m
Gas channel width and depth	1.0×10^{-3}m
Bipolar plate width	5.0×10^{-4}m
Gas diffusion layer thickness	3.0×10^{-4}m
Catalyst layer thickness	1.29×10^{-5}m
Cell temperature	70 C

The first important parameter, which should be explained, is temperature distribution especially along the cell width. The temperature affects the various factors of the fuel cell. As it is clear from Figs. 5, 6, 7 the temperature at the regions besides the bipolar plates is lower; because bipolar plates are good thermal conductors and cause the better heat transfer; this fact

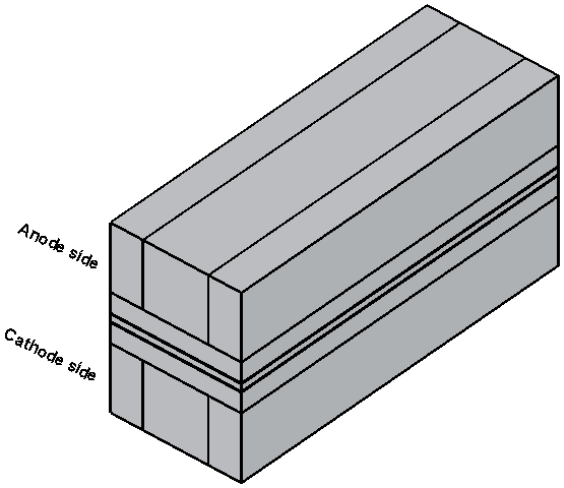

Fig. 3a Computational domain of numerical model

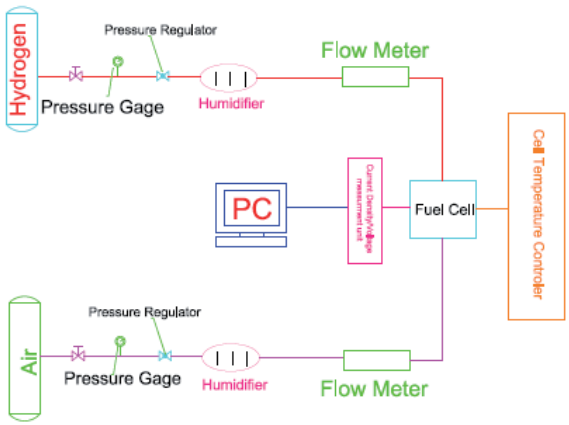

Fig. 3b PEMFC experimental set-up

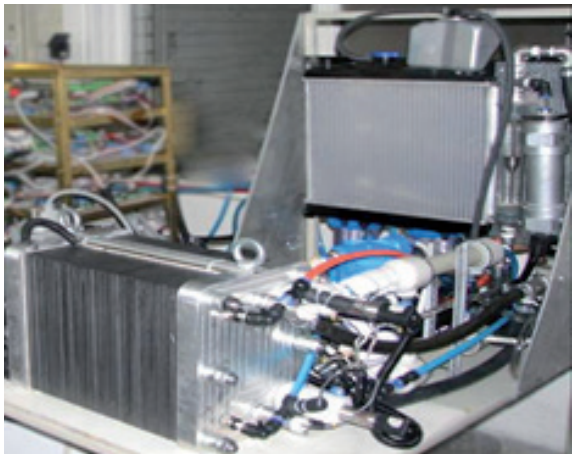

Fig. 3c Empirical testing case study (1.2 kW)

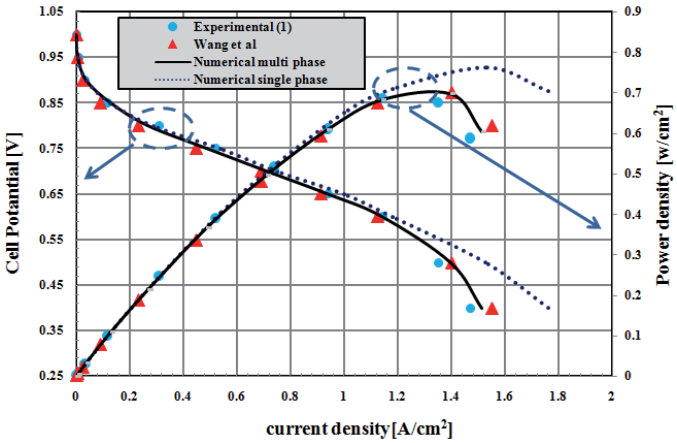

Fig. 4 Numerical results and experimental data comparison

leads to temperature reduction at the shoulder regions. The slightly temperature decrease along the flow direction is almost because of water magnitude and its distribution. The electro chemical reaction occurring in the cathode catalyst layer has two significant roles: water formation and temperature rise (so the cathode side temperature is higher than anode side).

Figure 8 indicates that water amount is growing up along the flow direction. This fact is the result of two important phenomena: water formation at the cathode catalyst layer; water transferring because of electro-osmotic drag from anode to cathode side. More water presence at the exit region of fuel cell cools the cell and decreases the temperature.

It is found that the water molecules at the inlet of the anode channel are transported mostly to the cathode by electro-osmotic drag but the electro-osmotic mass flux decreased along the channel. As shown in the Fig. 9, the back diffusion amount was much smaller than the electro-osmotic mass flux. Therefore the net water mass across the membrane is directed from anode to cathode side.

The Eq. (18) states that anode water activity is inversely related to temperature. Since the temperature is decreasing along the flow direction, consequently the anode water activity is increasing (Fig. 10). In addition, the water in the anode catalyst layer is responsible for transporting the hydrogen protons to the cathode side so its value should be reduced along the flow direction from inlet to outlet (Fig. 11); and since the oxygen amount in the longitudinal direction reduces (its consumption increases) and the water amount increases; more H^+ should be transported by water molecules. The lower the cell voltages the more water molecules transfer from anode to cathode.

The governing parameters of fuel cell; are highly dependent on each other. One of these important parameters is membrane protonic conductivity. This factor is excessively dependent on temperature (inversely) and anode water activity (directly).

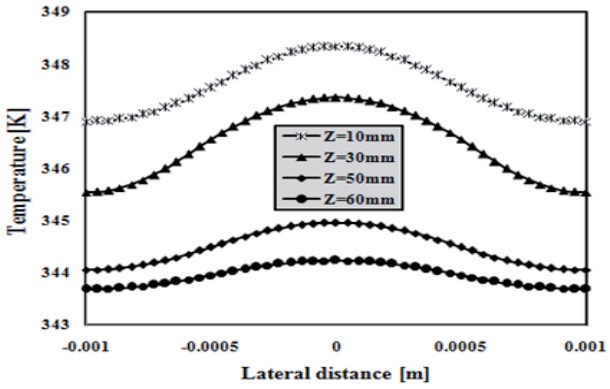

V=0.4[V]

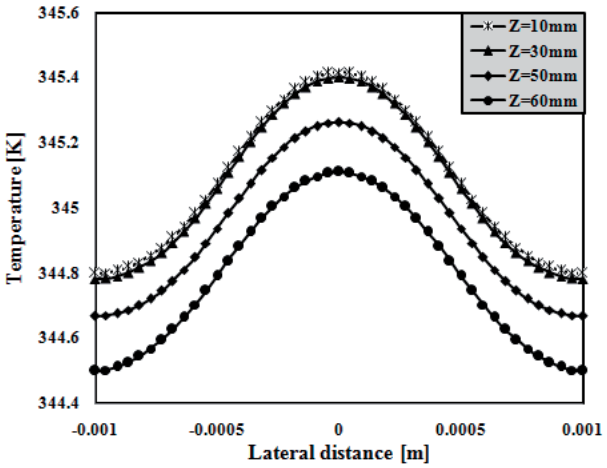

V=0.6[V]

Fig. 5 Temperature at cathode catalyst layer and membrane interface

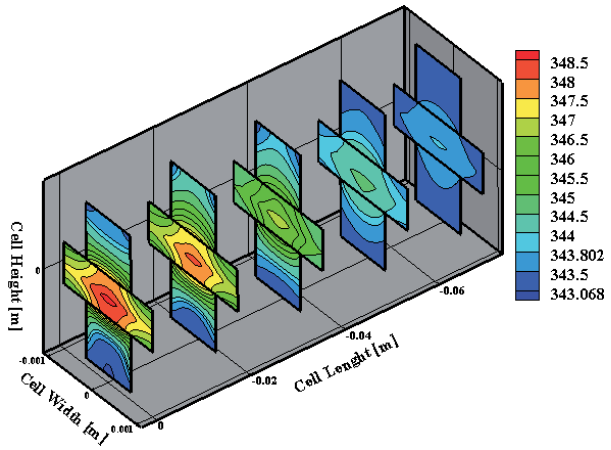

Fig. 6 Temperature [K]distribution contour at different cross sections at V=0.4[V]

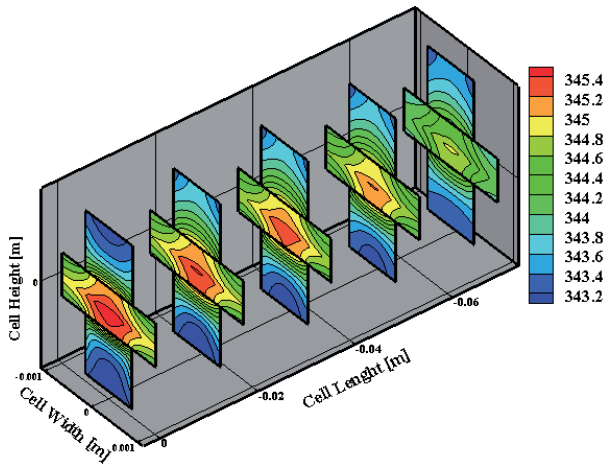

Fig. 7 Temperature [K] distribution contour at different cross sections at V=0.6[V]

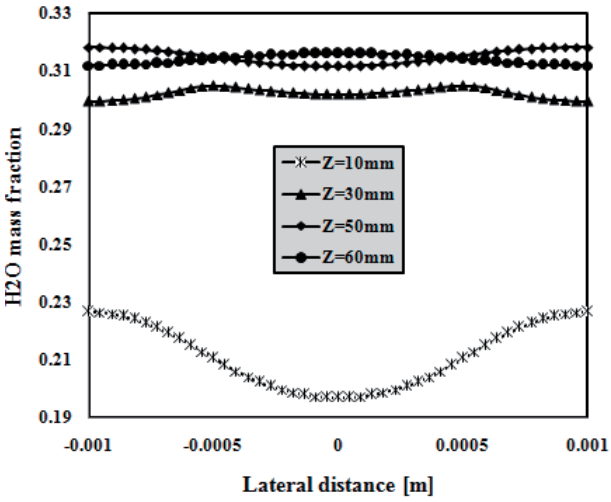

V=0.4[V]

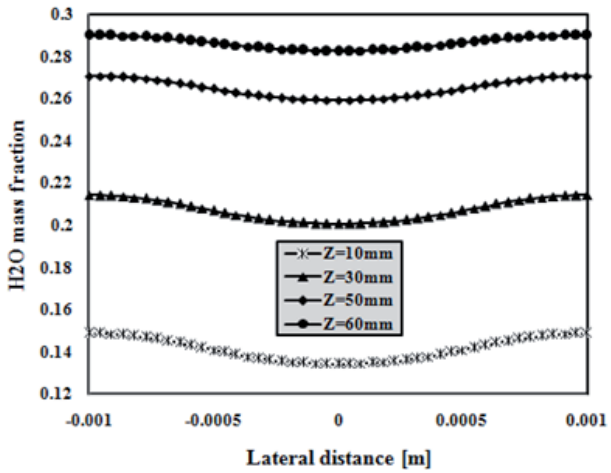

V=0.6[V]

Fig. 8 Water mass fraction at cathode catalyst layer and membrane interface

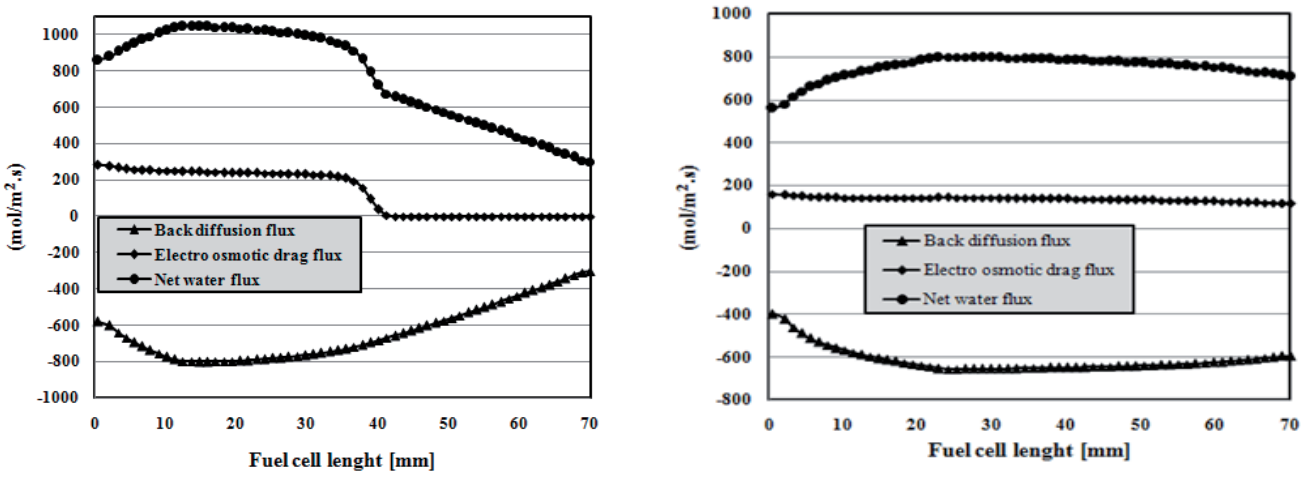

V=0.4[V] V=0.6[V]

Fig. 9 Water flux along the fuel cell

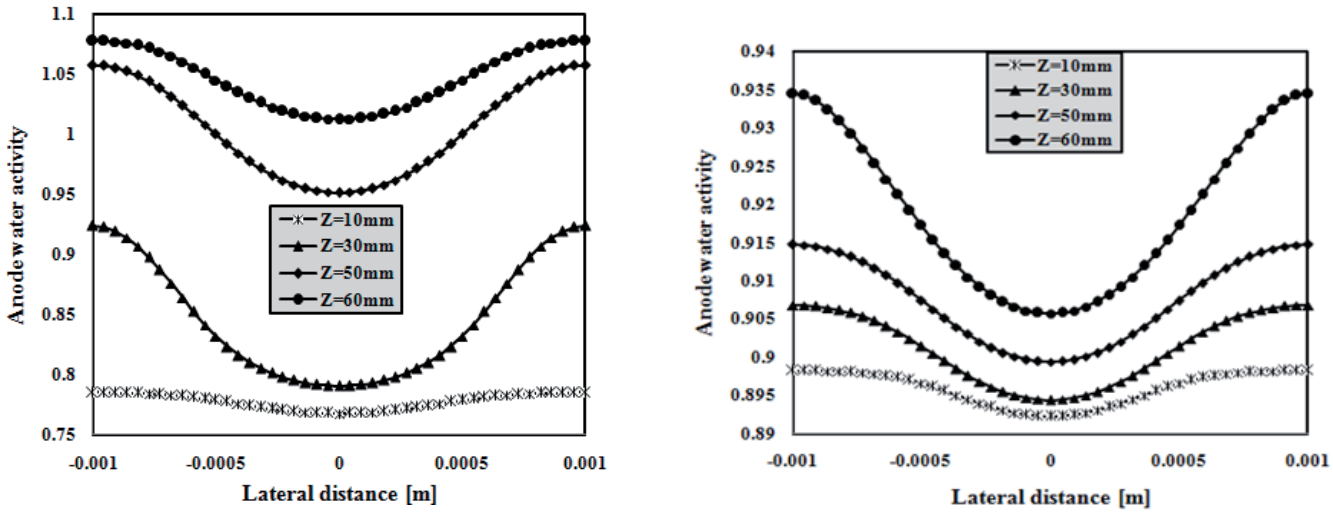

V=0.4[V] V=0.6[V]

Fig. 10 Anode water activity at anode catalyst layer and membrane interface

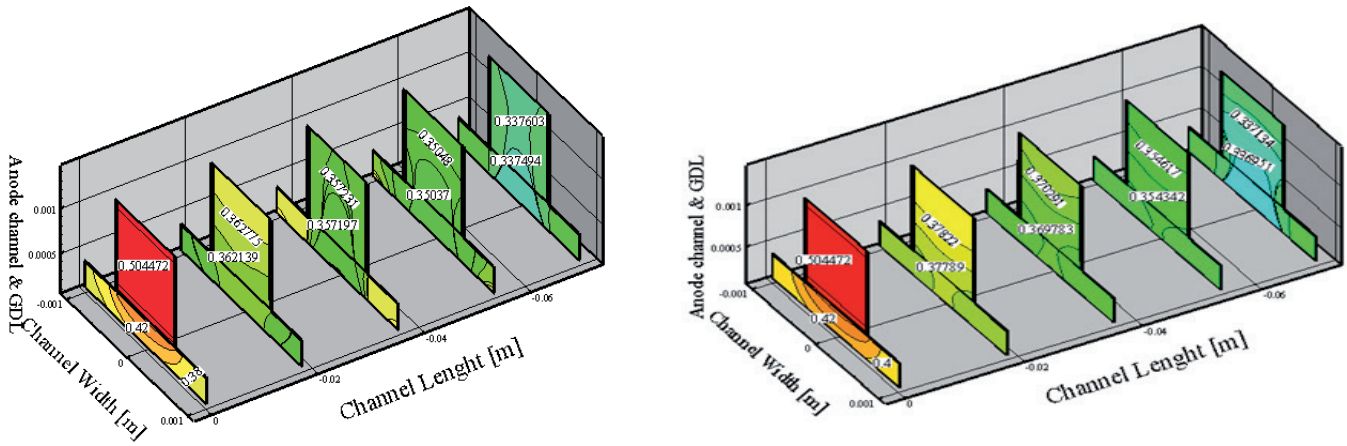

Fig. 11 Anode side water distribution at different planes of channel and GDL (0.4 V (Above) and 0.6 V (Below))

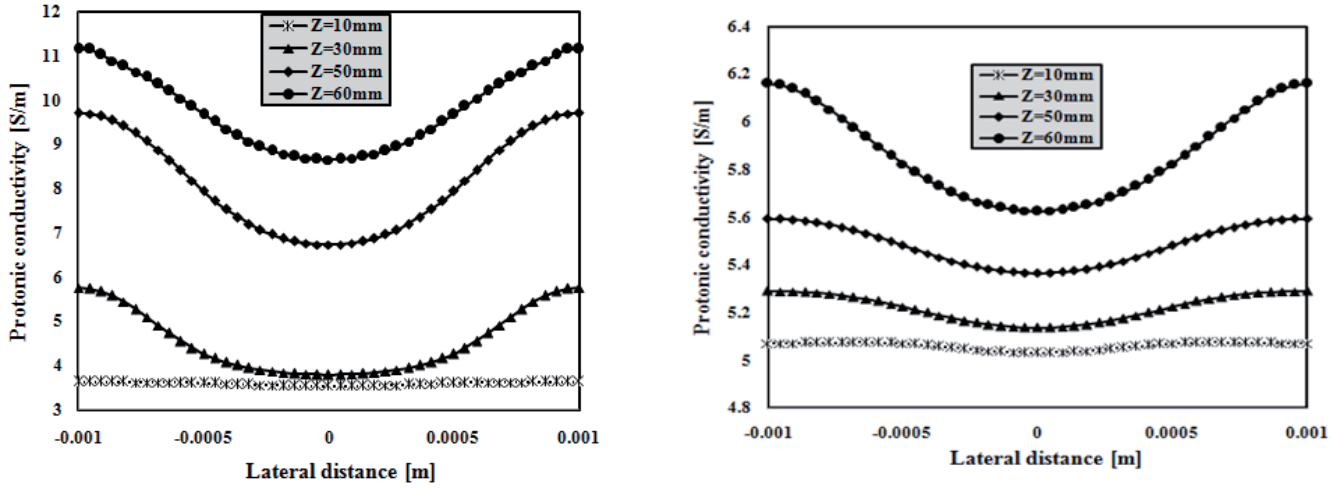

V=0.4[V] V=0.6[V]

Fig. 12 Protonic conductivity at anode catalyst layer and membrane interface

So its magnitude at shoulder region is higher than channel region (Fig. 12).

Figures 13, 14 illustrates the current density distribution at the interface of cathode catalyst and membrane. Current density indeed is electron flux in the cell and while electrons flow through the solid phase (solid phase of gas diffusion and catalyst layers), they want to traverse the shortest path to achieve the bipolar plates. So its value is higher at the shoulder region. In addition, current density amount dwindles along the flow direction. As it is mentioned before, water increasing along the cathode catalyst layer (especially at low voltages or high current densities) blocks the pores of porous mediums and consequently prevents the oxygen reaching to the reaction area. This fact leads to current density reduction along the flow direction.

According to Eq. (23) ohmic losses is directly related to membrane thickness(t_m) and current density (I). It is also inversely related to membrane protonic conductivity (σ_m).

$$R_{ohm} = \frac{t_m}{\sigma_e} \rightarrow \eta_{ohm} = IR_{ohm} \qquad (23)$$

One of parameters which affected by the oxygen distribution is cathode over potential. Where ever the fuel cell faces with lack of oxygen (which reason was discussed before and illustrated in Fig. 17), the cathode over potential is high (which is illustrated in Fig. 18).

Oxygen and water mass fraction distributions along the cathode catalyst and membrane interface are presented in Figs. 19-22. As mentioned before, oxygen amount (due to its consumption) decreases and water magnitude (due to its formation) increases.

It is clear that for V=0.4, 0.5 [V], oxygen gradually approaches to zero and water reaches to its maximum value and remains constant; because at these voltages, extra water blocks the pores of the gas diffusion layer and hampers the oxygen penetration to the cathode catalyst layer (concentration loss). Extra produced water has an important role in cooling fuel cell (temperature reduction), as shown in Fig. 23. As it can be obtained from results, there is a logical dependence between all of the operating parameters of fuel cell.

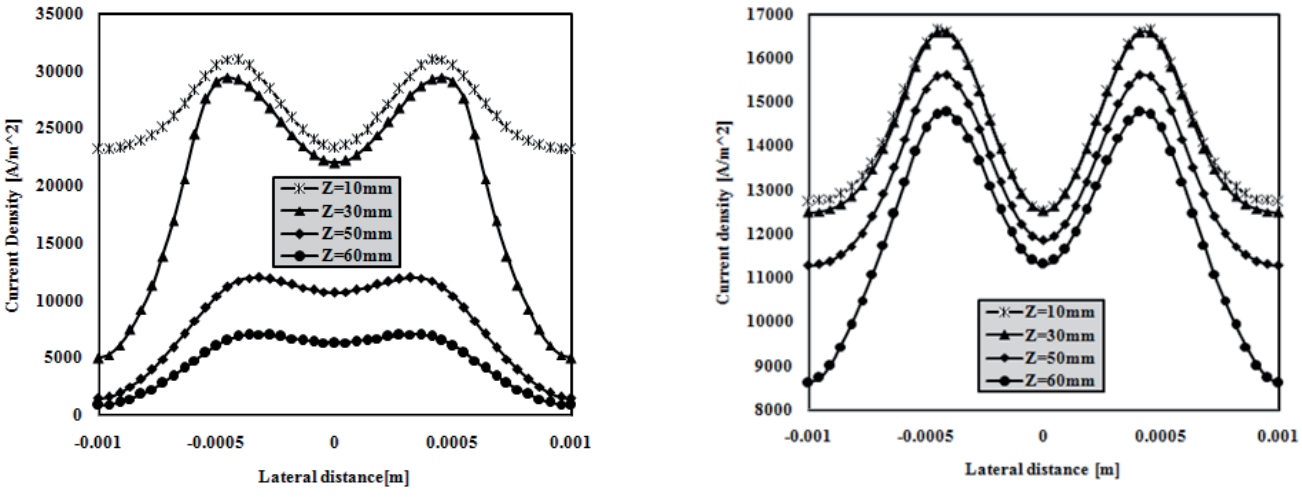

V=0.4[V] V=0.6[V]

Fig. 13 Current density magnitude at cathode catalyst later and membrane interface

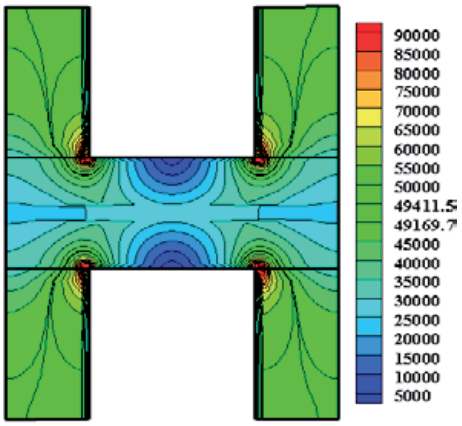

V=0.4[V] at Z=0mm

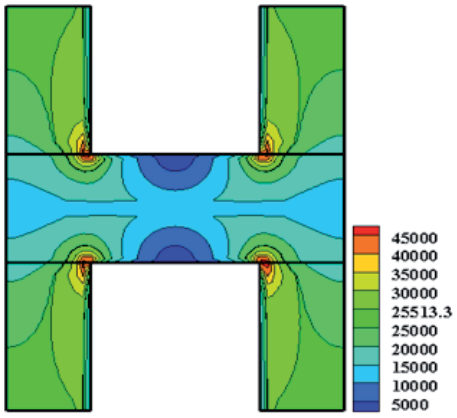

V=0.6[V] at Z=0mm

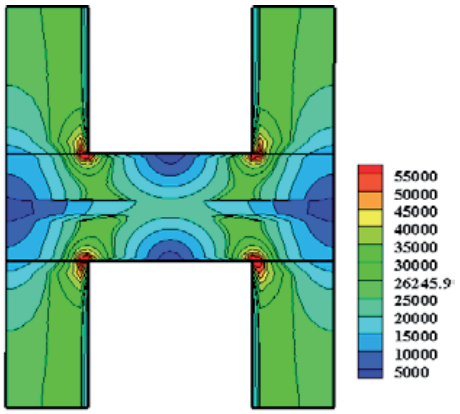

V=0.4[V] at Z=36mm

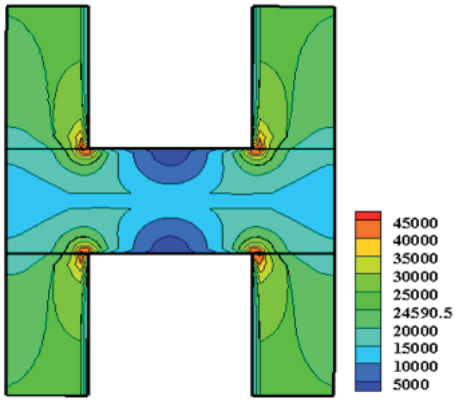

V=0.6[V] at Z=36mm

Fig. 14 Current density distribution at different cross sections

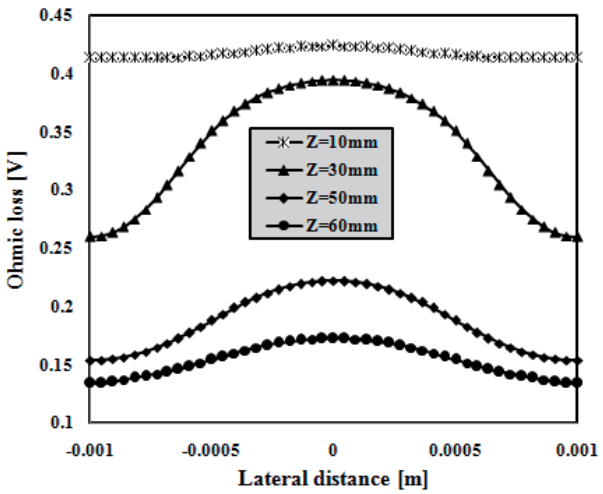

V=0.4[V]

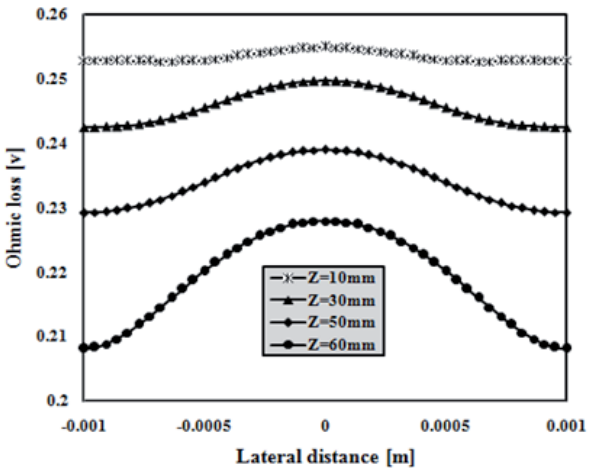

V=0.6[V]

Fig. 15 Ohmic loss at cathode catalyst later and membrane interface

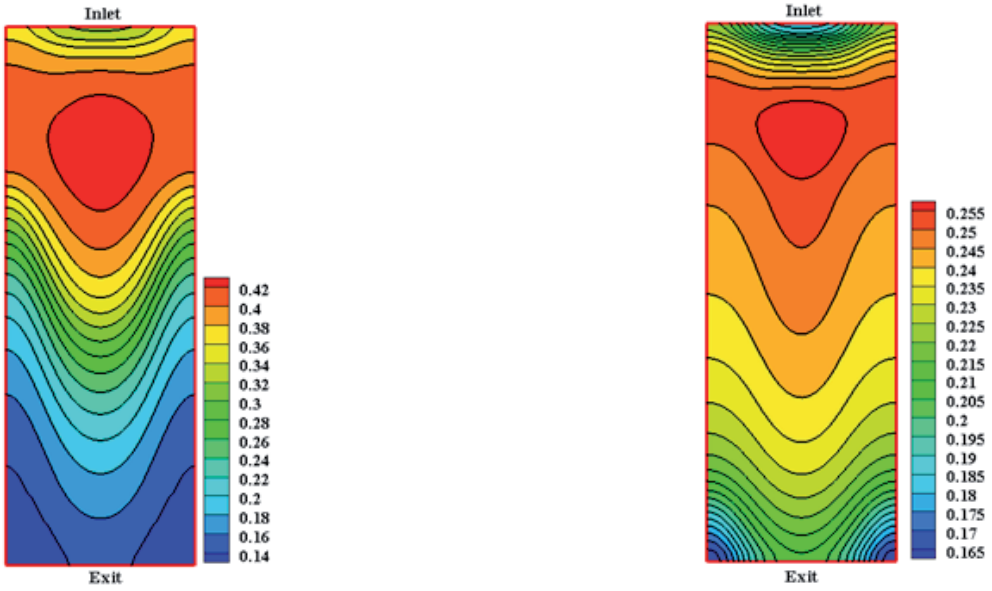

V=0.4[V] V=0.6[V]

Fig. 16 Ohmic loss contour at cathode catalyst layer and membrane interface

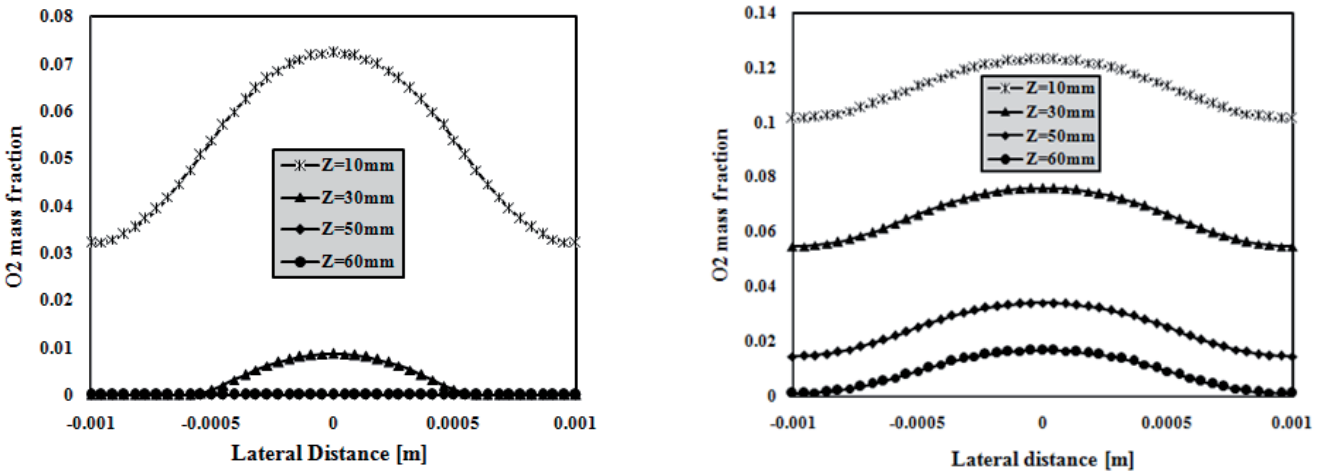

V=0.4[V] V=0.6[V]

Fig. 17 Oxygen mass fraction at cathode catalyst layer and membrane interface

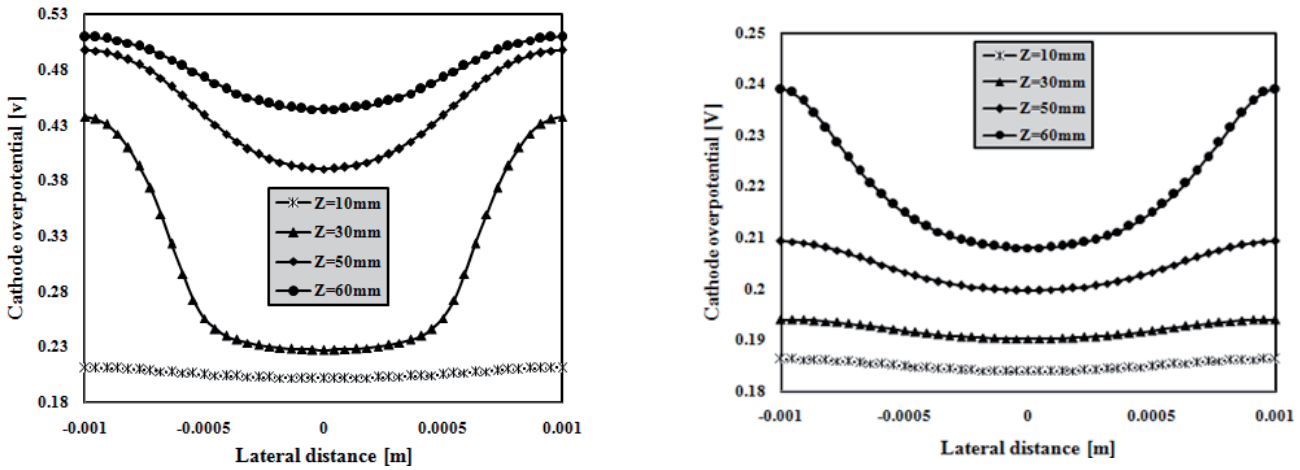

V=0.4[V] V=0.6[V]

Fig. 18 Cathode over potential at cathode catalyst layer and membrane interface

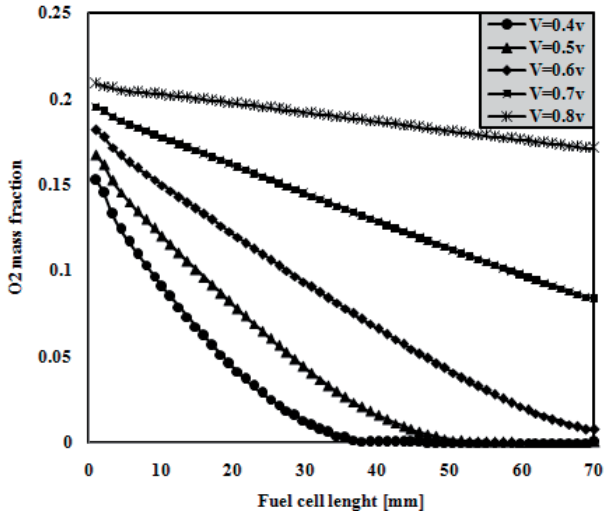

Fig. 19 Oxygen mass fraction along the cell at cathode catalyst layer and membrane interface

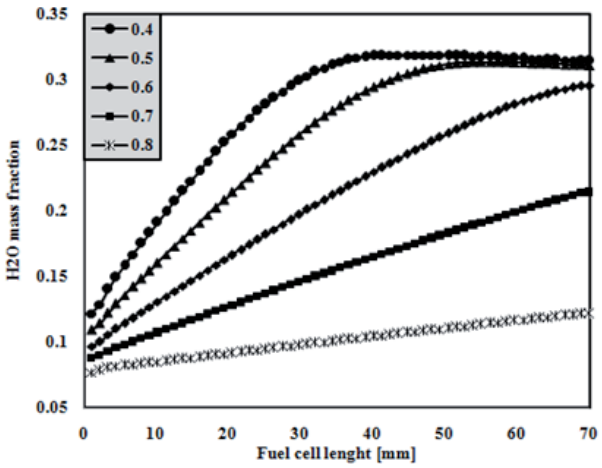

Fig 20 Water mass fraction along the cell at cathode catalyst layer and membrane interface

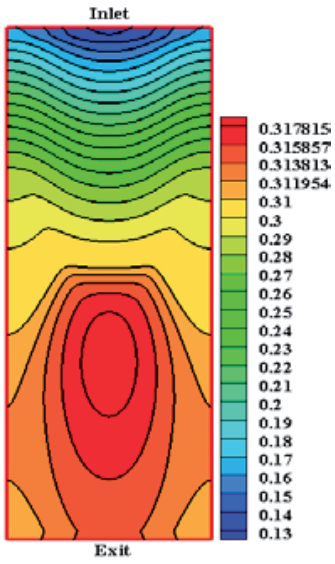

V=0.4[V]

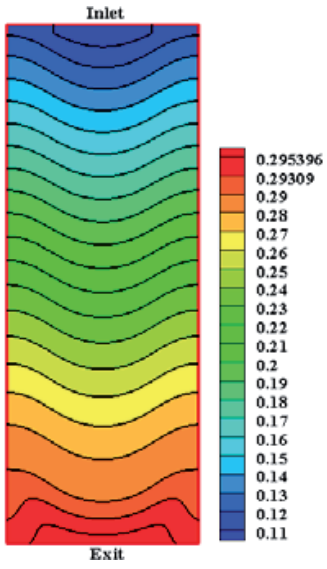

V=0.6[V]

Fig. 21 Water mass fraction contour along the cell at cathode catalyst layer and membrane interface

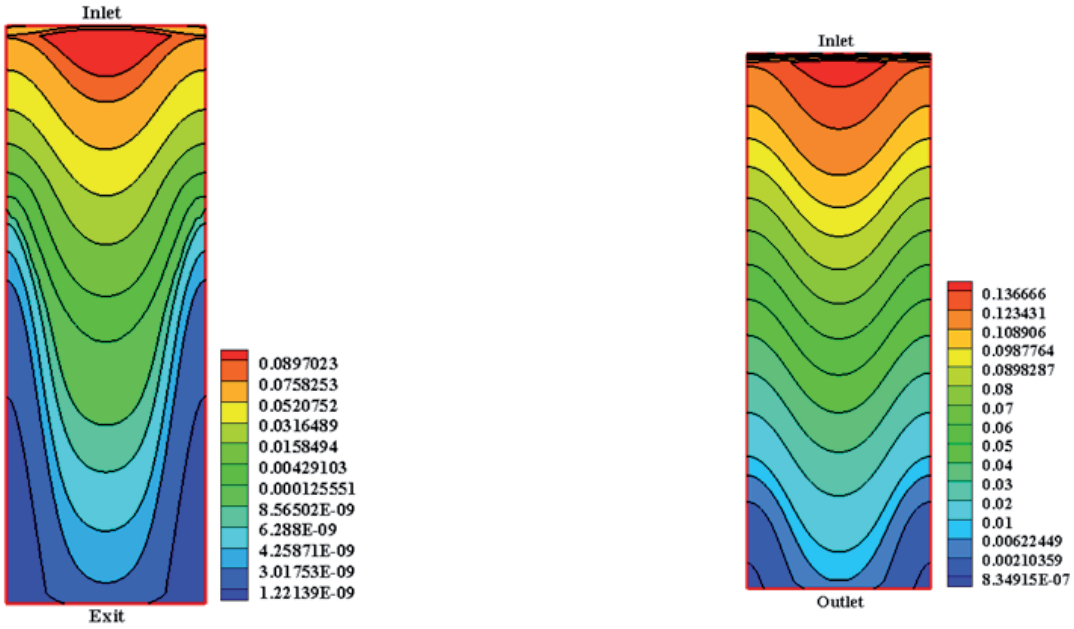

Fig. 22 Oxygen mass fraction contour along the cell at cathode catalyst layer and membrane interface

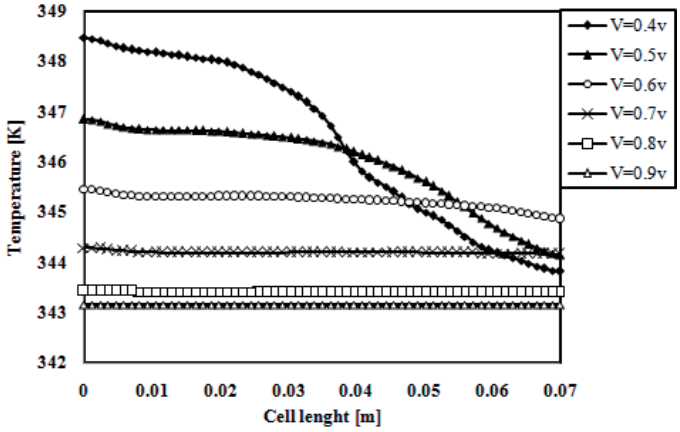

Fig. 23 Temperature distribution along the cell for different cell voltages at cathode catalyst layer and membrane interface

2 Effect of step-like gas channel

In this section the effect of step-like gas channel on the PEMFC performance is investigated in more detail. Figure 24 present the schematic of the case study at the lateral side. Table 2 presents geometrical configuration of step-like prominence.

Step like prominences yield to notable increasing in the velocity which velocity increasing front their part leads to improvement of the species distribution. These prominences give the channel nozzle like effect by reducing the gas flow cross section area. This effect accelerates the transferring of the reactant gas to the reaction area also it leads to the reactants distribute more uniform and better than base model (case without prominences). Figure 25 shows polarization diagram of two cases. It is clear that the case with prominences produces more current density in same condition than base model.

Table 2 Presents geometrical configuration of step-like prominence.

Value	Magnitude (mm)
a	23.33
b	0.67
c	0.33

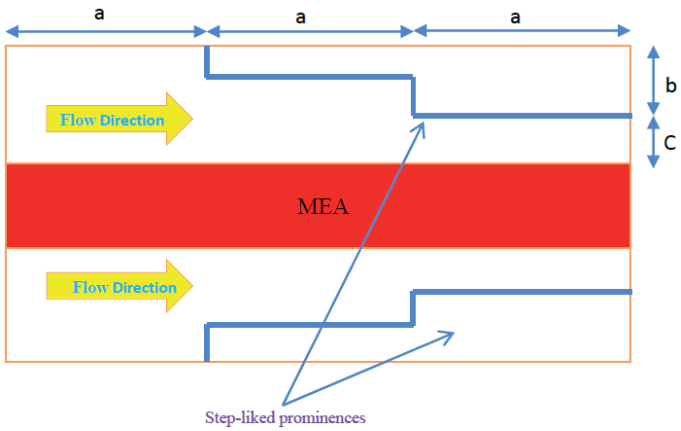

Fig. 24 schematic of step-like gas channel case (lateral view).

Figure 26 indicates velocity distribution of two cases in the gas channel. As it is observed, nozzle like effect of prominences leads to significant increasing in the velocity magnitude.

Figures 27 and 28 show the temperature distribution of two cases.

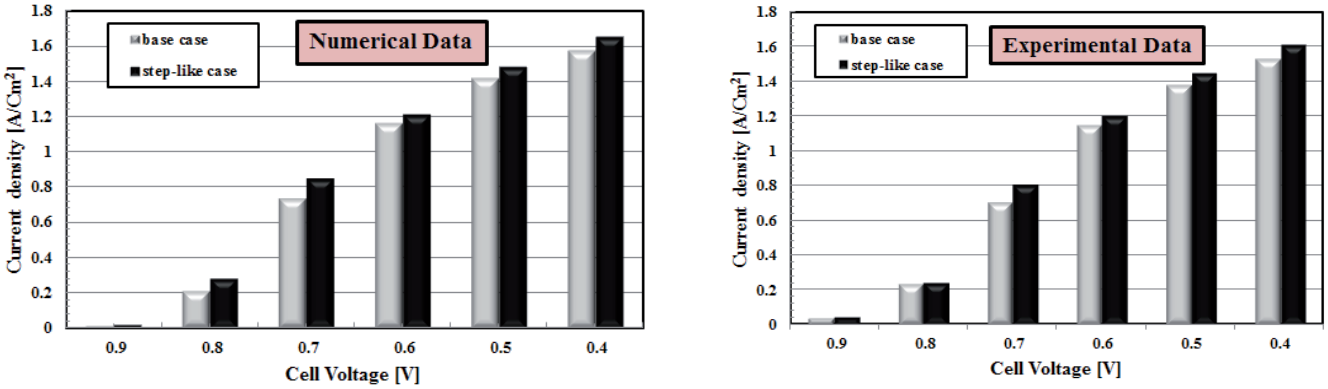

Fig. 25 Comparison the polarization diagram of two cases.

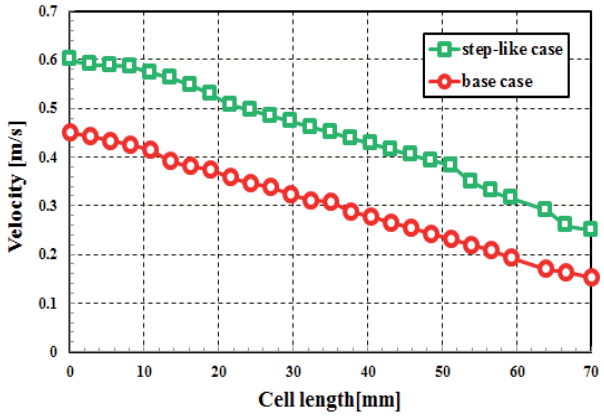

Fig. 26 Comparison velocity magnitude in the gas channel

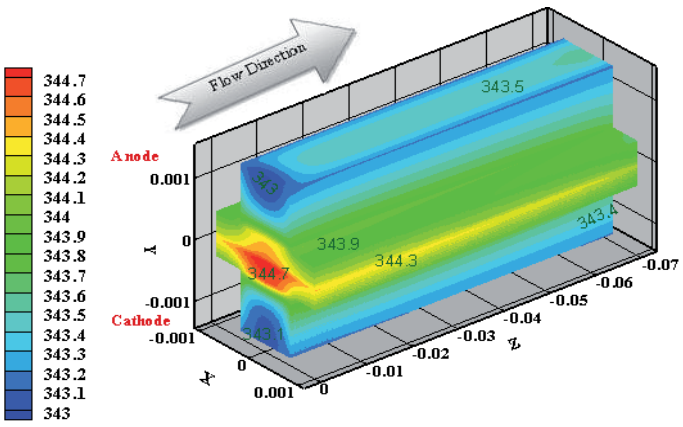

Fig. 27 Temperature distribution of base case (K)

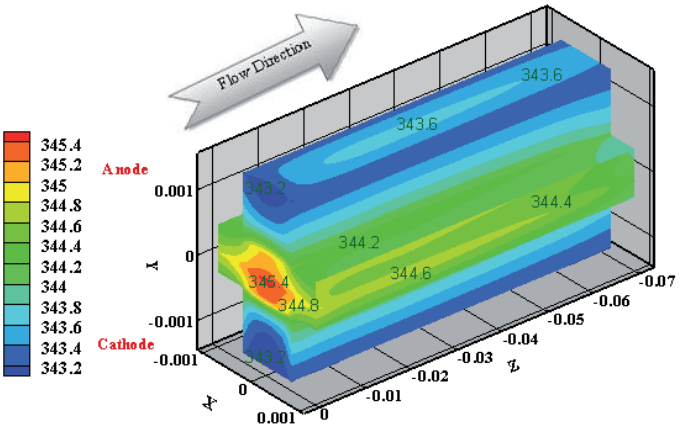

Fig. 28 Temperature distribution of step-like case (K)

3 Conclusions

In this article a three dimensional computational fluid dynamics model of a Proton Exchange Membrane Fuel Cell (PEMFC) with straight flow channels has been simulated. Also to verifying the accuracy of numerical results an in-house experimental test was performed. In present research, some parameters such as oxygen consumption, water production, temperature distribution, ohmic losses, anode water activity, and cathode over potential and the fuel cell performance for straight single cell were investigated in more details.

The temperature affects the various factors of the fuel cell. The at the regions besides the bipolar plates is lower; because bipolar plates are good thermal conductors and cause the better heat transfer; so the bipolar geometrical designing width better materials can be the important problems to study. In addition, electrons flow through the bipolar to the external circuit to produce electrical power. So the current density magnitude is higher at the shoulder regions; this fact affects the species and other important parameters distribution inside the cell.

On the other hand, the numerical simulations reveal that these important operating parameters are highly dependent to each other and the fuel cell efficiency is affected by the kind of species distribution. So for especial uses in desirable voltages, for preventing from the unwilling losses, these numerical results can be useful.

In this work at the following the effect of posing the step-like prominence in the gas channel was studied experimentally and numerically. The results reveal that these type of prominences yield to noticeable increasing in the velocity magnitude in the channels and this increase of velocity conduct species better and more uniform to the reaction area.

Nomenclature

a	Water activity
C	Molar concentration [mol m^{-3}]
D	Mass diffusion coefficient [m^2 s^{-1}]
F	Faraday constant [C mol^{-1}]
I	Local current density [A m^{-2}]
J	Exchange current density [A m^{-2}]
K	Permeability [m^2]
M	Molecular mass [kg mol^{-1}]
n_d	Electro-osmotic drag coefficient
P	Pressure [Pa]
R	Universal gas constant [J mol^{-1} K^{-1}]
T	Temperature [K]
t	Thickness
u	Velocity vector
V_{cell}	Cell voltage
$_{oc}$	Open-circuit voltage
W	Width
Y	Mass fraction
atm	Pressure Unit (atmosphere)
m	Meter
R	Resistance
h	Enthalpy

Greek Letter

α	Water transfer coefficient
ε_{eff}	Effective porosity
ρ	Density [kg m^{-3}]
ϕ_e	Electrolyte phase potential (varies from -1 to 1) [v]
μ	Viscosity [kg $m^{-1}s^{-1}$]
σ_m	Membrane conductivity [1.$ohm^{-1}m^{-1}$]
λ	Water content in the membrane
ξ	Stoichiometric ratio
η	Over potential [v]
λ_{eff}	Effective thermal conductivity [w $m^{-1}k^{-1}$]

Subscripts and superscripts

a	Anode
c	Cathode
ch	Channel
k	Chemical species
mem	Membrane
MEA	Membrane electrolyte assembly
ref	Reference value
sat	saturated
w	Water

Acknowledgements

This research was sponsored by Renewable Energy Organization of Iran.

References

[1] Arasti, M. R., Moghaddam, N. B. "Use of technology mapping in identification of fuel cell sub-technologies." *International Journal of Hydrogen Energy.* 35. pp. 9516-9525. 2010. DOI: 10.1016/j.ijhydene.2010.05.071

[2] Sadeghzadeh, K., Salehi, M. B. "Mathematical analysis of fuel cell strategic technologies development solutions in the automotive industry by the TOPSIS multi-criteria decision making method." *International Journal of Hydrogen Energy.* 36. pp. 13272–13280. 2011. DOI: 10.1016/j.ijhydene.2010.07.064

[3] Zaidi, S. M. J., Rahman, S. U., Zaidi, H. H. "R&D activities of fuel cell research at KFUPM." *Desalination.* 209. pp. 319–327. 2007. DOI: 10.1016/j.desal.2007.04.046

[4] Khorasani, M. R. A., Asghari, S., Mokmeli, A., Shahsamandi, M. H., Imani, B. F. "A diagnosis method for identification of the defected cell(s) in the PEM fuel cells." *International Journal of Hydrogen Energy.* 35. pp. 9269-9275. 2010. DOI: 10.1016/j.ijhydene.2010.04.157

[5] Costamagna, P., Srinivasan, S. "Quantum jumps in the PEMFC science and technology from the 1960s to the year 2000: part I. Fundamental scientific aspects." *Journal of Power Sources.* 102. pp. 242-252. 2001. DOI: 10.1016/s0378-7753(01)00807-2

[6] Rismanchi, B., Akbari, M. H. "Performance prediction of proton exchange membrane fuel cells using a three-dimensional model." *International Journal of Hydrogen Energy.* 33. pp. 439-448. 2008. DOI: 10.1016/j.ijhydene.2007.07.046

[7] Yaghini, N., Nordstierna, L., Martinelli, A. "Effect of water on the transport properties of protic and aprotic imidazolium ionic liquids – an analysis of self-diffusivity, conductivity, and proton exchange mechanism." *Physical Chemistry Chemical Physics*. 20 pp. 9266–9275. 2014. DOI: 10.1039/c4cp00527a

[8] Siahrostami, S., Björketun, M. E., Strasser, P., Greeley, J., Rossmeisl, J. "Tandem cathode for proton exchange membrane fuel cells." *Physical Chemistry Chemical Physics*. 23. pp. 9326-9334. 2013. DOI: 10.1039/c3cp51479j

[9] Mokmeli, A., Asghari, S. "An investigation into the effect of anode purging on the fuel cell performance." *International Journal of Hydrogen Energy*. 35. pp. 9276–9282. 2010. DOI: 10.1016/j.ijhydene.2010.03.079

[10] Jang, J.-H., Yan, W.-M., Shih, C.-C. "Numerical study of reactant gas transport phenomena and cell performance of proton exchange membrane fuel cells." *Journal of Power Sources*. 156. pp. 244-252. 2006. DOI: 10.1016/j.jpowsour.2005.06.029

[11] Seo, S.-J., Woo, J.-J., Yun, S.-H., Lee, H.-J., Park, J.-S., Xu, T., Yang, T.-H., Lee, J., Moon, S.-H. "Analyses of interfacial resistances in a membrane-electrode assembly for a proton exchange membrane fuel cell using symmetrical impedance spectroscopy." *Physical Chemistry Chemical Physics*. 46. pp. 15291-15300. 2010. DOI: 10.1039/c0cp00662a

[12] Yan, W.-M., Li, H.-Y., Chiu, P.-C., Wang, X.-D. "Effects of serpentine flow field with outlet channel contraction on cell performance of proton exchange membrane fuel cells." *Journal of Power Sources*. 178. pp. 174-180. 2008. DOI: 10.1016/j.jpowsour.2007.12.017

[13] Bernardi, D. M., Verbrugge, M. W. "Mathematical Model of a Gas Dissusion Electrode Bonded to a Polymer Electrolyte." *AIChE Journal*. 37 (8). pp. 1151-1163. 1991. DOI: 10.1002/aic.690370805

[14] Bernardi, D. M., Verbrugge, M. W. "A Mathematical Model of the Solid-Polymer-Electrolyte Fuel Cell." *Journal of Electrochemical Society*. 139 (9). pp. 2477-2491. 1992. DOI: 10.1149/1.2221251

[15] Fuller, T. F., Newman, J. "Water and Thermal Managament in Solid-Polymer-Electrolyte Fuel Cells." *Journal of Electrochemical Society*. 140 (5). pp. 1218-1225. 1993. DOI: 10.1149/1.2220960

[16] Nguyen, T. V., White, R. E. "Water and heat management model for proton-exchange-embrane fuel cells." *Journal of the Electrochemical Society*. 140. pp. 2178-2186. 1993. DOI: 10.1149/1.2220792

[17] Baschuk, J. J., Li, X. "Modelling of polymer electrolyte membrane fuel cells with variable degrees of water ‡ooding." *Journal of Power Sources*. 86. pp. 181-195. 2000. DOI: 10.1016/s0378-7753(99)00426-7

[18] Gurau, V., Liu, H., Kakac, S. "Two-Dimensional Model for Proton Exchange Membrane Fuel Cells." *AIChE Journal*. 44 (11). pp. 2410-2422. 1998. DOI: 10.1002/aic.690441109

[19] Dutta, S., Shimpalee, S., Van Zee, J. W. "Numerical prediction of mass-exchange between cathode and anode channels in a PEM fuel cell." *International Journal of Heat and Mass Transfer*. 44. pp. 2029–2042. 2001. DOI: 10.1016/s0017-9310(00)00257-x

[20] Ahmadi, N., Rezazadeh, S., Mirzaee, I., Pourmahmoud, N. "Three-dimensional computational fluid dynamic analysis of the conventional PEM fuel cell and investigation of prominent gas diffusion layers effect." *Journal of Mechanical Science and Technology*. 26 (8). pp. 1-11. 2012. DOI: 10.1007/s12206-012-0606-1

[21] Pourmahmoud, N., Rezazadeh, S., Mirzaee, I., Faed, S. M. "A computational study of a three-dimensional proton exchange membrane fuel cell (PEMFC) with conventional and deflected membrane electrode assembly." *Journal of Mechanical Science and Technology*. 26 (9). pp. 2959-2968. 2012. DOI: 10.1007/s12206-012-0708-9

[22] Wang, L., Husar, A., Zhou, T., Liu, H. "A parametric study of PEM fuel cell perfomances." *International Journal of Hydrogen Energy*. 28 (11). pp. 1263-1272. 2003. DOI: 10.1016/S0360-3199(02)00284-7

[23] Patankar, S. V. "*Numerical Heat Transfer and Fluid Flow.*" McGraw-Hill, 1980.